

Development and Modeling of Differentially Heat-Strengthened Rail Welding: Welding and Local Heat Treatment Modeling

N. A. Kozyrev^a, *, R. A. Shevchenko^a, A. A. Usol'tsev^a, A. N. Prudnikov^a, and L. P. Bashchenko^a

^aSiberian State Industrial University, Novokuznetsk, Kemerovo oblast, 654007 Russia

*e-mail: kozyrev_na@mtsp.sibsiu.ru

Received December 24, 2019; revised January 24, 2020; accepted January 31, 2020

Abstract—During the manufacturing of continuous welded rail track, the problem of the local hardened points in the welded joint during rail joint welding is resolved by using local heat treatment of the welded joint. As a result, the quenching structure formation is excluded. However, the appearance of new heat-affected zones with reduced hardness is possible. During operation, such rails are characterized by increased tread surface wear in these areas and rail flattening at the welded joint, which is the main reason for retiring the rails from service earlier than the guaranteed service life. A new technology based on the dependence of the structural component dispersion (primarily perlite and carbide particles formed in the process of rail butt welding) is proposed for the steel composition and cooling conditions. The cooling rate has a decisive influence on the dispersion degree of the ferrite-cementite structure formed during the austenite decomposition. During the welding rail process, the granular perlite formation is possible in a butt weld in areas with a temperature ranging within points Ac_1 and Ac_m . To determine these critical temperatures, thermodynamic calculations were performed using the Thermo-Calc® software (TCFE database) allowing the chemical composition of the samples obtained by spectrometry. The iron-carbon state diagrams for rail steel 76KhSF with the minimum and maximum alloying element content according to GOST R 51685–2013 are modeled. To obtain the minimum number of sections with reduced hardness, it is possible to weld rails using shot discontinuous flash welding. In order to eliminate the formation of defective areas with a quenching structure, it is possible to control the cooling of the welded joint by contact heating. Temperature distribution measurement during welding according to given modes and controlled cooling confirms the theoretical conclusions.

Keywords: rails, flash welding, heat treatment, current, impulse, welding mode, hardness, heat-affected zone

DOI: 10.3103/S0967091220030067

INTRODUCTION

The Russian Federation's railway industry has much strategic value. This link to its economic system ensures the stable operation of industrial enterprises and the timely delivery of vital goods to the most remote areas of the country, as well as being the most affordable transportation for millions of citizens. According to Russian Railways in 2019, the main rail tracks mileage was one of the longest in the world and amounts to over 124 thousand km. One of the main structural elements of railways are rails. Currently, the railways of the Russian Federation and abroad are abandoning the sectional track laying (bolted-type rail connection). One of the main drawbacks of the sectional track is the presence of a rail joint that promotes the formation of defects and premature rail decommissioning. The possibility of making a continuous railway track is a positive approach for the development of new technologies. It should be considered that the railway track operation in the country takes place in difficult climatic and operational conditions (there

is a common type of tracks in the country, not as in European countries which are separate for industrial and passenger railways).

Welded joints are weak sections of the continuous welded railway track for all types of movement (express and high-speed railway operations, heavy haul railroads). In 2018, 56% of rail fractures occurred due to welded joint fractures; and 15% of defective rails were revealed in the welded joint zone. This was due to a change in the microstructure uniformity in the welded joint zones and thermal impact; unfavorable internal residual stress distribution; creation of welding conditions for the internal defect formation, which are stress concentrators and weaken the rail section with a welded joint; rail contraction in the welded joint zone with subsequent deflection formation during operation. The problem of creating rails with an endurance of more than 1500–2000 million tons is resolved only with the comprehensive optimization of metallurgical quality (metal matrix structure, residual stress distribution, linearity) and the development of new welding technologies.

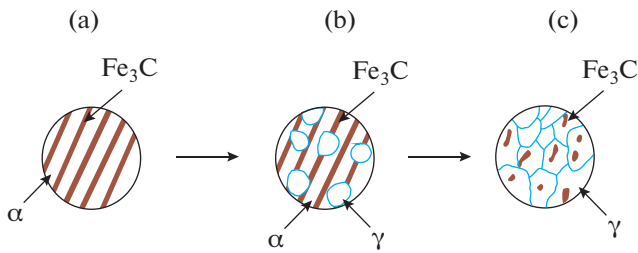


Fig. 1. Formation process of cementite spheroidization centers in the HAZ during weld heating: (a) the initial rail metal structure; (b) the growth of austenite sites; (c) the undissolved cementite, which later becomes the center of cementite spheroidization.

Presently, rail welded joints are a weak point of a welded continuous track, their warranty life is three times less than the service life of rails, and there is a tendency to increase the rail removal from the track due to welding defects and post-welding rail heat treatment. To improve operational performance in the Russian Federation, welded rail joints after welding are subjected to obligatory heat treatment at induction plants in order to exclude the formation of quenching structures (martensite and bainite), which cause additional stresses and cracks that lead to rail destruction. However, the local heat treatment of the welded joint leads to the expansion and emergence of new heat-affected zones (HAZ) in comparison with the zones formed by rail flash welding without heat treatment.

Currently, electric-arc, thermite, closed-gap and electric resistance welding are used worldwide for manufacturing continuous railway tracks. Electric-arc rail welding is mainly used on industrial and low-duty tracks. Since it is inefficient, the quality of the obtained joints does not meet modern requirements [1, 2]. Thermite welding, which is widespread abroad, has a relatively low reliability of welded rail joints and, accordingly, low technical and economic indicators of the life cycle, which is why it is not widely used in Russia [3]. Closed-gap welding makes it possible to obtain high mechanical properties of the welded joint. However, this type of welding is characterized by low productivity and high economic costs [4]. The most widespread type in Russia has been electric resistance rail welding due to the reliability of the obtained joints, productivity and economic efficiency [5]. At the same time, the currently developed methods of rail welding, especially those operating on high-speed railways, do not fully satisfy the requirements for the welded joint quality.

The transition from heat-hardened rails to differentially heat-hardened ones from rolling heat (to increase hardenability) led to an increase in the chromium content in rail steel [6]. In electric resistance welding, intense heating, implemented by discontinuous flashing with subsequent rapid cooling, promotes the formation of quenching structures at the location

of microscopic volumes with a high chromium content. Martensite sections are stress concentrators and lead to the development of fatigue cracks and brittle fracture.

The formation problem of local hardened areas in the process of continuous rail track welding is resolved by using the obligatory local heat treatment of the welded joint, which eliminates the formation of quenching structures. However, new HAZ with reduced hardness may appear in comparison with the electric resistance rail welding without heat treatment. During operation, the rails welded in this way are characterized by increased tread surface wear in these areas and rail flattening at the welded joint.

In pearlitic steel rails, a decrease in hardness in the heat affected zone is associated with the formation of granular perlite [7, 8], but the formation mechanism of this structure is usually not discussed. This is often considered as an obvious consequence of the delivered heat during welding. The study of this process will make it possible to give recommendations on minimizing the negative consequences of the thermal welding cycle.

The formation process of low hardness areas is similar to the process of spheroidize annealing used in production to reduce hardness and improve the steel cutting ability [9]. To obtain granular perlite (cementite in the form of rounded grains), spheroidize annealing is carried out, which consists of steel heating to a temperature slightly above the eutectoid temperature (point A_{c1}), retardation and subsequent cooling. Upon steel heating slightly above the critical point A_{c1} , the initial austenite nuclei are formed in its structure by shearing while maintaining coherent boundaries. The austenite nucleus occurs at the interphase between ferrite and cementite (Fig. 1a). As a result of this transformation, low-carbon austenite is formed (Fig. 1b). Cementite dissolves in the low-carbon austenite formed by the shear mechanism, and the carbon content in austenite approaches equilibrium. The growth of austenite sites as a result of polymorphic $\alpha \rightarrow \gamma$ transformation proceeds faster than the cementite dissolution. Excess structural components do not completely pass into solution. Upon subsequent cooling, they become centers of cementite spheroidization (Fig. 1c).

The introduction of chromium, vanadium, molybdenum, tungsten, and other carbide-forming elements into steel delays the austenitization process due to the formation of alloyed cementite or carbides of alloying elements that are more difficult to dissolve in austenite [10–16].

With subsequent cooling, cementite coagulation occurs in the areas of the remaining undissolved carbide and coarsening of cementite grains—spheroidization. Fig. 2 schematically shows two types of eutectoid transformations: the formation of lamellar and granular perlite.

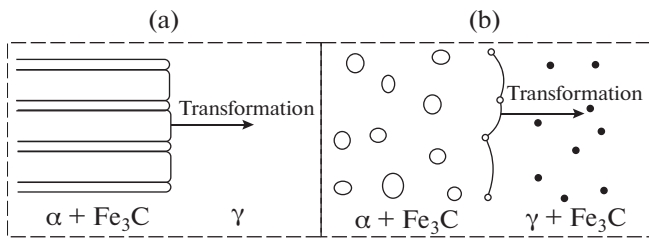


Fig. 2. Schematic representation of the formation of lamellar (a) and granular (b) perlite (austenite (γ) composing ferrite (α), cementite Fe_3C).

The perlite dispersion depends on the steel composition and cooling conditions, and retarded cooling contributes to the enlargement of carbides and vice versa. The cooling rate, acting on diffusion transformations, has a significant effect on the structure and properties of the ferrite-cementite mixture, which is formed during the austenite decomposition. In the rail welding, the granular perlite formation occurs in areas whose temperature reaches values that fall within the interval between the critical points Ac_1 and Ac_m .

RESULTS AND DISCUSSION

To determine the critical temperatures for Ac_1 and Ac_m of the studied rail steel, thermodynamic calculations were performed using the Thermo-Calc[®] software (TCFE database) with allowance for the chemical composition of the samples obtained by spectrometry (Table 1).

Using the results of the chemical composition as input data for thermodynamic calculations, the critical point positions and the phase equilibrium region were simulated for rail steel (Fig. 3). For steel with a carbon content of 0.77%, calculations show that the complete conversion to ferrite and cementite will occur at a temperature of about 720°C and there will

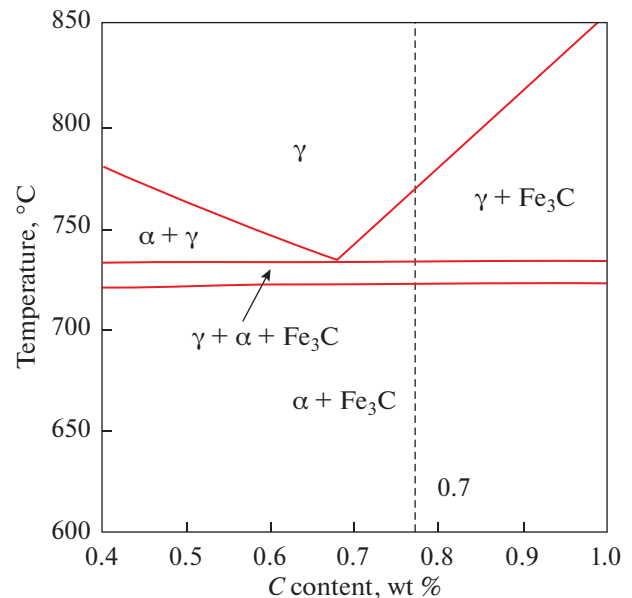


Fig. 3. Iron–Carbon state diagram obtained using thermodynamic calculations showing the predicted equilibrium between the ferrite (α), austenite (γ) and cementite (Fe_3C) phases.

be three phases between temperatures of 720 and 730°C. Above 730°C (up to about 770°C), there is an intercritical region (austenite and cementite).

During this study, the change in the critical point position and the phase equilibrium region were simulated for rail steel 76KhSF with the minimum (Fig. 4a) and maximum (Fig. 4b) content of alloying elements according to GOST R 51685 –2013.

For steels with a carbon content of 0.71 and 0.82%, as a result of the calculation, it was determined that the complete conversion to ferrite and cementite will occur at a temperature of about 725°C for two alloys and there will be three phases up to temperatures of

Table 1. Chemical composition of the samples

Sample	Chemical composition, %															
	C	Mn	Si	Cr	V	P	S	Ni	Al	Cu	Ti	Mo	Nb	Sn	O	H, ppm
1	0.76	0.77	0.53	0.37	0.04	0.010	0.010	0.08	0.003	0.12	0.002	0.006	0.002	0.005	0.0010	0.90
2	0.77	0.77	0.53	0.37	0.04	0.012	0.009	0.08	0.003	0.10	0.003	0.007	0.002	0.005	0.0009	0.08
3	0.76	0.77	0.53	0.37	0.04	0.010	0.010	0.08	0.003	0.12	0.002	0.006	0.002	0.005	0.0010	0.90
4	0.77	0.77	0.53	0.37	0.04	0.012	0.009	0.08	0.003	0.10	0.003	0.007	0.002	0.005	0.0009	0.08
5	0.77	0.80	0.56	0.38	0.04	0.008	0.006	0.06	0.002	0.10	0.002	0.006	0.002	0.005	0.0013	1.10
6	0.76	0.78	0.55	0.38	0.04	0.010	0.006	0.07	0.003	0.10	0.002	0.005	0.002	0.004	0.0012	0.90
7	0.76	0.77	0.53	0.37	0.04	0.009	0.005	0.07	0.003	0.11	0.002	0.005	0.001	0.005	0.0009	1.00
8	0.76	0.78	0.55	0.38	0.04	0.010	0.006	0.07	0.003	0.10	0.002	0.005	0.002	0.004	0.0012	0.90
9	0.77	0.80	0.56	0.38	0.04	0.008	0.006	0.06	0.002	0.10	0.002	0.006	0.002	0.005	0.0013	1.10

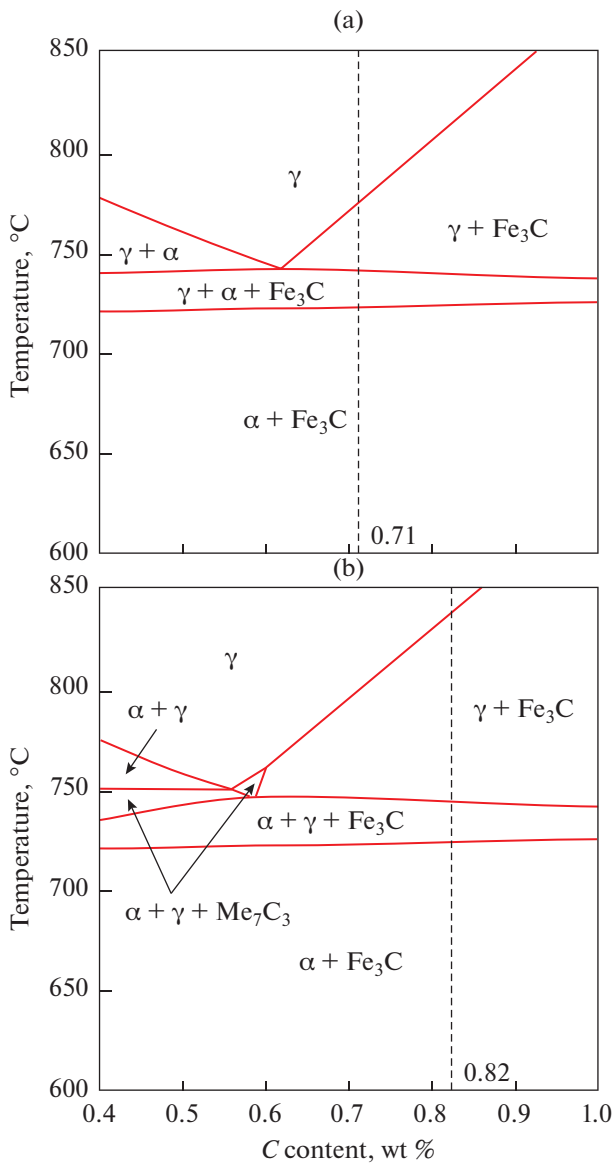


Fig. 4. Iron–Carbon state diagrams obtained using thermodynamic calculations showing the predicted equilibrium between the ferrite (α), austenite (γ), and cementite (Fe_3C) phases: (a) C = 0.71%; Mn = 0.75%; Si = 0.25%; Cr = 0.50%; V = 0.08%; (b) C = 0.82%; Mn = 1.25%; Si = 0.60%; Cr = 1.25%; V = 0.15%.

740 and 745°C. Above 745°C, the alloy has an intercritical region (austenite and cementite) up to 775 and 840°C for steel 76KhSF with the minimum and maximum alloying elements, respectively (Figs. 4a, 4b).

As a result of the thermodynamic analysis, it was determined (Figs. 3, 4) that steel 76KhSF is hypereutectoid. The zone formation with reduced hardness in the welded joint is inevitable as a result of the temperature gradient created by welding. With an increase in the content of steel alloying elements, the temperature region between critical points A_{c1} and A_{cm} increases,

which leads to an increase in the length of the zone with reduced hardness in the welded joint.

There is the possibility of minimizing these areas with shot welding. It is obvious that continuous flash welding will have a greater coverage of the zone with reduced hardness compared to the discontinuous flash method. However, upon rapid welded joint heating, which is provided by discontinuous flashing and subsequent intensive cooling of the HAZ, a high-strength layer with a martensite structure is formed at the site of microscopic volumes with a high content of chromium, nickel and carbon. This problem in the process of making a continuous track during rail welding is resolved by the obligatory welded joint local heat treatment. Local heat treatment is carried out using induction plants. As a result, new HAZ are formed, which have sections with reduced hardness of even greater extent compared to electric flash welding.

To obtain the minimum length of the section with reduced hardness, it is possible to conduct shot discontinuous flash rail welding. Furthermore, in order to prevent defect formation as quenching structures, it is possible to control the cooling of the welded joint using contact heating. During welding, using a transformer from a track welding machine is proposed as a power source for contact heating.

The experimental research is based on the planned experiment method [17]. As a model, a linear polynomial of the following form was chosen:

$$\tilde{y} = b_0 + \sum_{i=1}^n b_i x_i + \sum_{i<j}^n b_{ij} x_i x_j,$$

where \tilde{y} is the optimization parameter; b_0 , b_i , b_{ij} are the coefficients; x_i are the variable factors; and $x_i x_j$ are the double factor interactions.

During the steel cooling process, the austenite transformation occurs only after its supercooling below temperature A_{r1} , which is explained by a change in the free phase energy and alloy structures during heating and cooling. During steel supercooling, austenite turns into plate perlite. With a small degree of austenite supercooling, perlite is formed in the temperature range. With a greater degree of supercooling in the temperature range, sorbitol is formed after austenite transformation. With even greater supercooling degrees, fine perlite comes out [18].

It is proposed to control metal cooling after welding by alternating electric current in predetermined conditions. The investigated parameters of controlled cooling are: X_1 —cooling time after upset (characterized by the cooling rate (degree of austenite supercooling) and threshold cooling temperature T_1); X_2 —heating time (characterized by threshold heating temperature T_2); X_3 —cooling time after heating (characterized by threshold cooling temperature T_1); X_4 —the number of heating pulses (characterized by the incubation

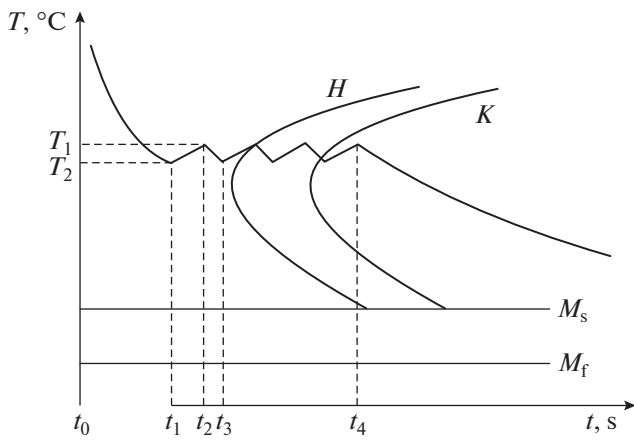


Fig. 5. Diagram of the austenite isothermal decomposition with controlled workpiece cooling after welding.

period of the austenite-perlite conversion). Fig. 5 shows a schematic graph of the controlled cooling.

Holding time (X_1) was selected so that the weld joint cools down to the temperature at which the required welded joint structure is formed. The current transmission pulses were set at a certain interval. Pulse duration (X_2) is determined by the temperature of the welded joint, which should not rise above the temperature values required for the formation of the required structure. The duration of interval (X_3) is selected so that the temperature of the weld joint does not fall below the temperature value at which the required welded joint structure is formed. The number of pulses (X_4) sets the time during which the average welded joint temperature is maintained, which is necessary for the formation of the required structure during welding.

The length and the decrease in hardness in the heat-affected zone obtained after welding were selected as the objective function.

To select the zero level of factors and the range of variation, the temperature distribution was calculated during welding and controlled cooling according to the procedure described in [19]. Table 2 presents the initial data for calculating the temperature distribution in the metal welded joint and heat affected zones. For the calculation, the following initial data were used: $v = 1$ mm/s—flash rate; $t = 10$ s—welding time; $\lambda = 0.2$ W/(mm °C)—steel thermal conductivity; $I = 11700$ A—current conducting through the workpiece; $R = 8.6 \times 10^{-7}$ Ohms—samples resistance; $\Delta\tau$ —current passage time (X_2), s; $A = 0.0172$ m²—surface area of the body through which heat is transferred; $T_0 = 20^\circ\text{C}$ —ambient temperature; $m = 0.315$ kg—mass of the heated metal volume; $c = 0.25$ kJ/(kg °C)—specific metal heat.

Figure 6 presents the calculation results of the temperature distribution from the welded joint center at

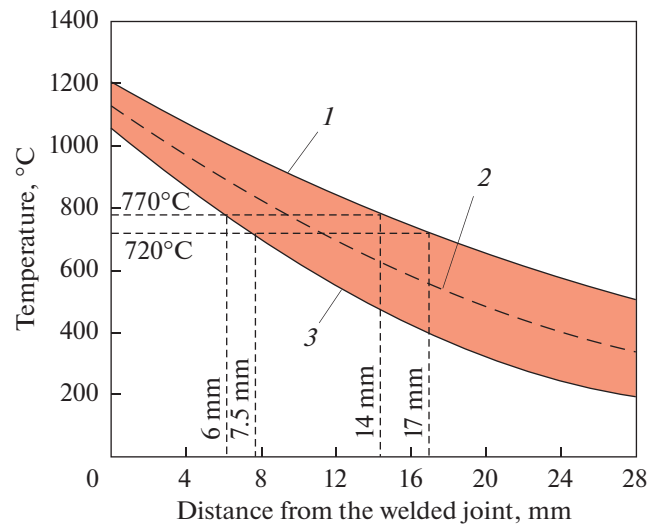


Fig. 6. Calculated temperature distribution at various welding and controlled cooling modes: 1–3 are the controlled cooling modes (Table 2).

the time of completion of welded joint AC heating. The factor variation levels are presented in Table 3.

Mode 2 was selected as the zero level of factors.

To search for optimal isothermal conditions, a full factorial experiment $N = 2 \times 3^k$ was carried out (Table 4). To eliminate a systematic error in determining the optimization parameters, randomization was performed using random number tables. The order of the tests was as follows: 8, 9, 2, 6, 5, 3, 7, 4, 1.

Table 2. Values of the controlled cooling parameters for calculating temperature distribution

Mode	Factor values			
	X_1 , s	X_2 , s	X_3 , s	X_4 , number of pulses
1	20.0	0.6	10	4
2	22.5	0.4	15	3
3	25.0	0.2	20	2

Table 3. Factor variation levels

Indicator	Factor values			
	X_1 , s	X_2 , s	X_3 , s	X_4 , number of pulses
Zero level x_0	22.5	0.4	15	3
Interval of variation h_j	2.5	0.2	5	1
Upper level (+1)	25	0.6	20	4
Lower level (-1)	20	0.2	10	2

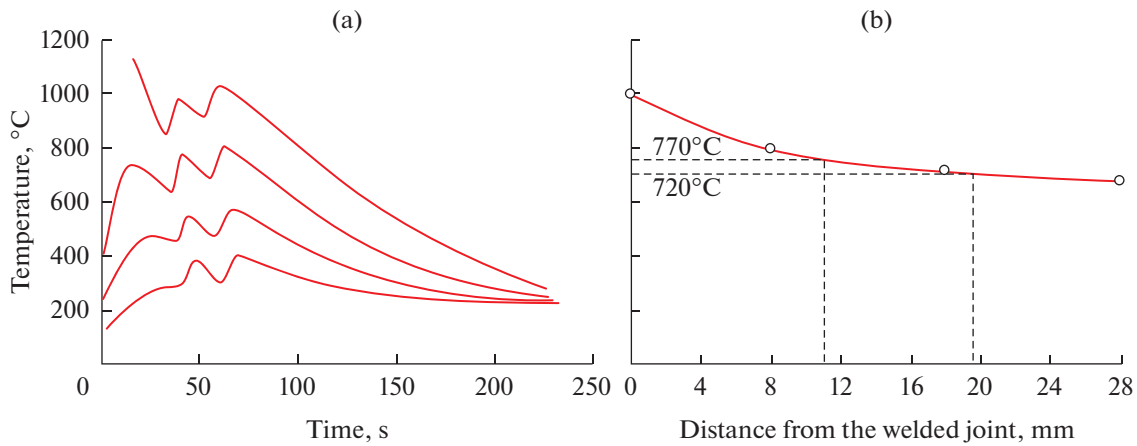


Fig. 7. Temperature distribution during sample 1 welding.

Using the technique described in [20], a measurement of the welding temperature distribution was carried out. The welding mode of laboratory samples was as follows: transformer tap 10; $K_{tr} = 65$; $U_2 = 5.76$ V; $I_2 = 11700$ A; $\Delta_{flash} = 10$ mm; $\Delta_{upset} = 4$ mm; $v = 1$ mm/s. The experiments were carried out according to the specified welding and controlled cooling mode (Table 4).

Figure 7 shows a thermal flash welding cycle followed by controlled cooling and the instantaneous temperature fields distribution in the heat-affected zone after the end of the controlled cooling cycle for sample 1 (the same data were determined for the other samples).

In accordance with the welding and controlled cooling modes, the heating process and subsequent pulse heating is 30.4 – 90.8 s, depending on the mode. On the thermal cycle diagrams of welded samples 1, 5–9, it is possible to observe heating up to 1020–1320°C and subsequent sharp cooling of the welded metal joint. This type of change in the welded joint

temperature leads to the quenching structure formation inside it.

In samples 1, 5–9, an analysis of the instantaneous temperature fields distribution in the heat-affected zone shows that the heat propagates from the short-term heating source to a greater distance relative to the welding heat propagation.

In samples 1, 5, 6, 9, the temperatures between critical points Ac_m (770°C) and Ac_1 (720°C) correspond to the maximum linear dimensions of this region (from 5 to 8.5 mm). In samples 2–4, 7, 8, the temperatures between critical points Ac_m and Ac_1 correspond to the minimum (from 2.5 to 3.2 mm) linear dimensions.

CONCLUSIONS

The use of local heat treatment of the welded rail joint by the flash welding method eliminates the formation of sections containing quenching structures. Local heat treatment leads to an increase in HAZ.

During rail structure welding, the granular perlite formation occurs in the sections with a temperature corresponding to the interval between points Ac_1 and Ac_m . Using thermodynamic calculations based on the Thermo-Calc® software, the temperatures of critical points Ac_1 and Ac_m and the equilibrium phases for various rail steel 76KhSF composition under consideration were determined.

In order to obtain the minimum length of the section with reduced hardness, it is possible to conduct shot rails welding by the flash method using a discontinuous method. In order to prevent defect formation as quenching structures, it is possible to control the cooling of the welded joint using contact heating. A rail welding machine transformer is recommended to be used as a power source for contact heating.

Table 4. Experiment planning matrix $N = 2 \times 3^k$

Sample	Factor values			
	X_1, s	X_2, s	X_3, s	$X_4,$ number of pulses
1	25 (+)	0.4 (0)	20 (+)	2 (–)
2	25 (+)	0.2 (–)	15 (0)	3 (0)
3	20 (–)	0.2 (–)	10 (–)	2 (–)
4	20 (–)	0.2 (–)	20 (+)	4 (+)
5	20 (–)	0.4 (0)	15 (0)	4 (+)
6	20 (–)	0.4 (0)	10 (–)	3 (0)
7	20 (–)	0.6 (+)	20 (+)	3 (0)
8	25 (+)	0.6 (+)	10 (–)	4 (+)
9	20 (–)	0.6 (+)	15 (0)	2 (–)

REFERENCES

1. Poznyakov, V.D., Kir'yakov, V.M., Gaivoronskii, A.A., Klapatyuk, A.V., and Shishikevich, O.S., Properties of welded joints of rail steel at electric arc welding, *Avtom. Svarka*, 2010, no. 8 (688), pp. 19–24.
2. Dahl, B., Mogard, B., Grefot, B., and Ulander, B., Repair of rails on-site by welding, *Svetsaren*, 1995, vol. 50, no. 2, pp. 10–14.
3. Rukavchuk, Yu.P., Rozhdestvenskii, S.A., and Etingen, I.Z., Defectiveness of joints at aluminothermic rail welding, *Put' Putevye Khoz.*, 2011, no. 4, pp. 26–27.
4. Gudkov, A.V. and Lozinskii, V.N., New technological and technical solutions in welding for railway transport: problems and judgments, *Vestn. Vseross. Nauchno-Issled. Inst. Zheleznodorozhn. Transp.*, 2008, no. 6, pp. 3–9.
5. Kalashnikov, E.A. and Korolev, Yu.A., Rail welding technology: trends in Russia and abroad, *Put' Putevye Khoz.*, 2015, no. 8, pp. 2–6.
6. Girsch, G., Keichel, J., Gehrman, R., Zlatnik, A., and Frank, N., Advanced rail steels for heavy haul applications-track performance and weldability, *Proc. 9th Int. Heavy Haul Conf. "Heavy haul and innovation development," Shanghai, June 22–25, 2009*, Shanghai, 2009.
7. Mutton, P., Cookson, J., Qiu, C., and Welsby, D., Microstructural characterization of rolling contact fatigue damage in flashbutt welds, *Wear*, 2016, vol. 366, pp. 368–377.
8. Leikin, A.E. and Rodin, B.I., *Materialovedenie. Uchebnik dlya mashinostroitel'nykh spetsial'nostei vuzov* (Materials Science: Manual for Machine Engineering Specialties of Higher Education Institutions), Moscow: Vysshaya Shkola, 1971.
9. Lakhtin, Yu.M. and Leont'eva, V.P., *Materialovedenie. Uchebnik dlya vysshikh tekhnicheskikh uchebnykh zavedenii* (Materials Science: Manual for Higher Education Engineering Institutions), Moscow: Mashinostroenie, 1990.
10. Oyama, T., Sherby, O.D., Wadsworth, J., and Walser, B., Application of the divorced eutectoid transformation to the development of fine-grained, spheroidized structures in ultrahigh carbon steels, *Scr. Metall.*, 1984, vol. 18, no. 8, pp. 799–804.
11. Nakano, T., Kawatani, H., and Kinoshita, S., Effects of Cr, Mo and V on spheroidization of carbides in 0.8% carbon steel, *Trans. Iron Steel Inst. Jpn.*, 1977, vol. 17, no. 2, pp. 110–115.
12. Zhang, G.H., Chae, J.Y., Kim, K.H., and Suh, D.W., Effects of Mn, Si and Cr addition on the dissolution and coarsening of pearlitic cementite during intercritical austenitization in Fe–1 mass % C alloy, *Mater. Charact.*, 2013, vol. 81, pp. 56–67.
13. Molinder, G., A quantitative study of the formation of austenite and the solution of cementite at different austenitizing temperatures for a 1.27% carbon steel, *Acta Metall.*, 1956, vol. 4, no. 6, pp. 565–571.
14. Hillert, M., Nilsson, K., and Torndahl, L.-E., Effect of alloying elements on the formation of austenite and dissolution of cementite, *J. Iron Steel Inst.*, 1971, vol. 209, no. 1, pp. 49–66.
15. Goune, M., Maugis, P., and Drillet, J., A criterion for the change from fast to slow regime of cementite dissolution in Fe–C–Mn steels, *J. Mater. Sci. Technol.*, 2012, vol. 28, no. 8, pp. 728–736.
16. Luzginova, N.V., Zhao, L., and Sietsma, J., The cementite spheroidization process in high-carbon steels with different chromium contents, *Metall. Mater. Trans. A*, 2008, vol. 39, pp. 513–521.
17. Kostin, V.N. and Tishina, N.A., *Statisticheskie metody i modeli: uchebnoe posobie* (Statistical methods and Models: Manual), Orenburg: Orenb. Gos. Univ., 2004.
18. Skugorova, L.P., *Materialy dlya sooruzheniya gazonefteprovodov i khranilishch: uch. posobie* (Materials for Construction of Oil and Gas Pipelines and Storage: Manual), Moscow: Nedra, 1989.
19. Shevchenko, R.A., Kozyrev, N.A., Shishkin, P.E., Kryukov, R.E., and Usol'tsev, A.A., Calculation of optimal modes of rails electrical contact welding, *Vestn. Gorno-Metall. Sekts. Ross. Akad. Estestv. Nauk, Otd. Metall.*, 2016, no. 37, pp. 175–180.
20. Shevchenko, R.A., Kozyrev, N.A., Kutsenko, A.I., Usol'tsev, A.A., and Kutsenko, A.A., Methodology of the study of isothermal annealing modes impact during rail steel welding, *Vestn. Sib. Gos. Ind. Univ.*, 2018, no. 4 (26), pp. 8–11.

Translated by A. Kolemesin

SPELL: 1. ok